Zbigniew ŁUKASIK[1], Andriy CZABAN[1], Andrzej SZAFRANIEC[1], Vołodymyr ŻUK[2]

University of Technology and Humanities in Radom, Faculty of Transport and Electrical Engineering (1), Lviv Polytechnic (2)

The mathematical model of the drive system with asynchronous motor and vertical pump

Abstract. The mathematical model of electric drive, which consists of deep groove asynchronous motor that rotates the axial pump, is substantiated, using the interdisciplinary modeling method, based on the modified Hamilton-Ostrogradsky's principle by expanding the known Lagrange function. Resulting differential equations are represented in normal Cauchy form and are integrated numerically.

Streszczenie. W pracy na podstawie interdyscyplinarnej metody modelowania, która opiera się na zmodyfikowanej zasadzie Hamiltona-Ostrogradskiego z uwzględnieniem rozszerzenia funkcji Lagrange'a opracowano model matematyczny układu napędowego, który składa się z głębokożłobkowego silnika asynchronicznego sprzęgniętego z pompą pionową. Równania różniczkowe stanu elektromechanicznego przedstawione są w postaci normalnej Cauchy'ego, które całkowane są za pomocą metod numerycznych. (Model matematyczny układu napędowego z silnikiem asynchronicznym i pompą pionową).

Keywords: Hamilton-Ostrogradsky's principle, Euler–Lagrange equation, electromechanical energy conversion, hydraulic drive.
Słowa kluczowe: zasada Hamiltona-Ostrogradskiego, równania Eulera-Lagrange'a, elektromechaniczne przetwarzanie energii, napęd hydrauliczny.

Introduction

Mathematical modelling of transient electrodynamics processes occurring in complex drive systems is an assignment that has not been completed yet. It is well known that in the aforementioned systems, sophisticated physical processes occur in the course of which electromagnetic energy is transformed into mechanical energy, which is next turned into hydraulic energy. In complex electromechanical-hydraulic high power system, either incorrect or inaccurate description of means of energy transformation may result with drive system failure.

This article describes mathematical modelling of transient dynamic processes of system comprising deep groove asynchronous motor which is coupled with vertical pump [10] by means of a fixed shaft. Such system is characterized by multiple transformation of energy, which makes analysis of electromechanical-hydraulic processes a complex issue. The very process itself is complicated by nature. Additionally, no one has yet designed mathematical model of vertical pumps integrated in electromechanical part of drive system [2], [3], [7], [9]. In consequence, in order to complete the above described assignment a comprehensive interdisciplinary knowledge in three scientific fields is required: electrical engineering, applied mechanics and hydrodynamics. For aforementioned complex systems it is recommended to apply interdisciplinary modelling methods, which significantly expands research capabilities [1], [5]. This method uses modified integral Hamilton-Ostrogradsky's principle by expanding Lagrange function with two components: dispersion forces energy and non-potential energy of external forces. It should be noted that expanded Lagrange function is obtained by analytical method.

This article aim is to design a mathematical model of complex drive system comprised of deep groove asynchronous motor coupled with vertical pump, and to analyse transient electromechanical-hydraulic processes.

Mathematical model of the system

Mathematical model of analysed object is presented in figure 1. Asynchronous motor AM is powered from power grid via air coil and it drives vertical pump which is a component of hydraulic network.

Extended Lagrange function of the proposed method takes the following form [1], [4], [6]:

$$(1) \qquad L^* = \tilde{T}^* - P^* + \Phi^* - D^*$$

where: L^* – modified Lagrange function, $\tilde{T}^*$ – kinetic coenergy, P^* – potential energy, Φ^* – dissipation energy, D^* – energy of external non-potential forces [1], [4], [11].
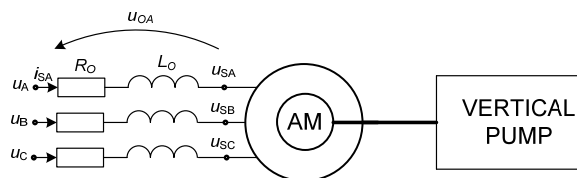
Fig.1. Drive system diagram

In order to calculate lagrangian components (1) the following generalized coordinates were introduced:
Electric charges in stator winding

$$q_{(1-3)} = Q_{SA}, Q_{SB}, Q_{SC},$$

Electric charges in rotor winding

$$q_{(4-6)} = Q_{RA}, Q_{RB}, Q_{RC},$$

Drive rotation angle

$$q_7 = \gamma,$$

Liquid volume

$$q_8 = V.$$

Referring to generalized speeds $\dot{q} \equiv dq / dt$, windings current values, flow rate and pump's rotational speed are determined:

$$\dot{q}_{(1-3)} = i_{SA}, i_{SB}, i_{SC},$$

$$\dot{q}_{(4-6)} = i_{RA}, i_{RB}, i_{RC},$$

$$\dot{q}_7 = \omega,$$

$$\dot{q}_8 = Q.$$

where: i – current, ω – drive rotational speed, Q – vertical pump flow rate.

When designing extended functional of operation by Hamilton-Ostrogradsky's, all parameters and functional relations of rotor of induction motor were recalculated to stator side [6].

Variation of functional of operation by Hamilton-Ostrogradsky's may be determined either in a conventional way according to [1], [4], [5] or using Lagrange theory, more precisely Euler- Lagrange'a equation [6], which simplifies calculations.

$$(2) \qquad \frac{d}{dt}\frac{\partial L^*}{\partial \dot{q}_i} - \frac{\partial L^*}{\partial q_i} = 0, \quad i = 1-7$$

Elements of non-conservative lagrangian for the system presented in figure 1 are determined by the following equations:

$$(3) \qquad \tilde{T}^* = \left[\tilde{T}_O^*\right] + \left[\tilde{T}_E^*\right] + \left[\tilde{T}_M^*\right] + \left[\tilde{T}_H^*\right] =$$

$$= \sum_{j=1}^{3} \left\{ \left[\frac{L_O i_{Sj}^2}{2}\right] + \left[\int_0^{i_{Sj}} \Psi_{Sj} di_{Sj} + \int_0^{i_{Rj}} \Psi_{Rj} di_{Rj}\right] \right\} +$$

$$+ \left[\frac{(J_1 + J_2)\omega^2}{2}\right] + \left[\frac{L_H Q^2}{2}\right];$$

$$(4) \qquad P^* = 0, \quad \Phi^* = \frac{1}{2}\sum_{j=1}^{3}\left\{\int_0^t R_{Sj} i_{Sj}^2 d\tau + \int_0^t r_{Sj} i_{Sj}^2 d\tau + \int_0^t r_{RLj} i_{Rj}^2 d\tau\right\} +$$

$$+ \frac{1}{2}\int_0^t R_H Q^2 d\tau, \quad j = A, B, C$$

$$(5) \quad D^* = \int_0^t \left(u_A i_{SA} + u_B i_{SB} + u_C i_{SC}\right)d\tau - \int_0^t \int_0^\omega M_P(\omega)d\omega d\tau.$$

where particular indices are:
O – air coil, E – motor, M – shaft, H – pump.
Ψ_{Sj}, Ψ_{Rj} – linked fluxes of stator and rotor, J_1, J_2 – motor and pump's moment of inertia, $\mathbf{r}_{Sj}, \mathbf{r}_{RLj}$ – resistance of stator and rotor head, $\mathbf{i}_{Sj}, \mathbf{i}_{Rj}$ – currents of stator and rotor, $\mathbf{u_j}$ – system power supply voltage, M_p – pump hydraulic torque, R_H, L_H – virtual resistance and inductance of pump and pipe [9].

Using Wit-Woodson theory, the following assumptions are made [1], [6]:

$$(6) \qquad M_{EM} = \frac{\partial\left[\tilde{T}_E^*\right]}{\partial\gamma}, \qquad u_{Rj} = -\frac{\partial\left[\tilde{T}_E^*\right]}{\partial Q_{Rj}}$$

$$(7) \qquad \rho g(H_2 - H_1) + p_O = \frac{\partial\left[\tilde{T}_H^*\right]}{\partial V}$$

$$(8) \qquad \frac{\partial}{\partial i_{kj}}\int_0^{i_{kj}} \Psi_{kj} di_{kj} = \Psi_{kj}, \qquad \frac{\partial}{\partial i_{ml}}\int_0^{i_{kj}} \Psi_{kj} di_{kj} \equiv 0$$

$$(9) \qquad k = S, R, \quad j = A, B, C, \quad i_{ml} \neq i_{kj}$$

where: $\boldsymbol{u}_R$ – matrix of motor cage voltage drops including displacement of currents in rotor winding [1], M_{EM} – motor starting torque, ρ – liquid density, p_0 – calculated pipe pressure, g – gravitational acceleration, $(H_2 - H_1)$ – liquid head difference.

Equations (3) – (5) are inserted into equation (2) which enables to obtain the following:

$$(10) \qquad \frac{d}{dt}\frac{\partial L^*}{\partial i_{Sj}} - \frac{\partial L^*}{\partial Q_{Sj}} = \frac{d}{dt}\frac{\partial}{\partial i_{Sj}}\left(\frac{L_O i_{Sj}^2}{2} + \int_0^{i_{Sj}} \Psi_{Sj} di_{Sj} + \right.$$

$$\left. + \frac{1}{2}\int_0^t R_O i_{Sj}^2 d\tau + \frac{1}{2}\int_0^t r_{Sj} i_{Sj}^2 d\tau - \int_0^t u_j i_{Sj} d\tau\right) - 0 = 0 ;$$

$$(11) \qquad \frac{d}{dt}\frac{\partial L^*}{\partial i_{Rj}} - \frac{\partial L^*}{\partial Q_{Rj}} = \frac{d}{dt}\frac{\partial}{\partial i_{Rj}}\left(\int_0^{i_{Rj}} \Psi_{Rj} di_{Rj} + \frac{1}{2}\int_0^t r_{Rj} i_{Rj}^2 d\tau\right) -$$

$$- \frac{\partial}{\partial Q_{Rj}}\left[\tilde{T}_E^*\right] = 0, \qquad j = A, B, C ;$$

$$(12) \qquad \frac{d}{dt}\frac{\partial L^*}{\partial \omega} - \frac{\partial L^*}{\partial \gamma} = \frac{d}{dt}\frac{\partial}{\partial \omega}\left(\frac{(J_1 + J_2)\omega^2}{2} + \right.$$

$$\left. + \int_0^t\int_0^\omega M_P(\omega)d\omega d\tau\right) - \frac{\partial\left[\tilde{T}_E\right]}{\partial\gamma} = 0 ;$$

$$(13) \qquad \frac{d}{dt}\frac{\partial L^*}{\partial Q} - \frac{\partial L^*}{\partial V} = \frac{d}{dt}\frac{\partial}{\partial Q}\left(\frac{L_H Q^2}{2}\right) + \frac{\partial\left[\tilde{T}_H^*\right]}{\partial V} = 0 .$$

Taking into account Kirchhoff's law, matrix-vector equation is obtained:

$$(14) \qquad \frac{d\mathbf{\Psi}_S}{dt} = \mathbf{u} - \mathbf{u}_O - \mathbf{r}_S\mathbf{i}_S, \qquad \frac{d\mathbf{\Psi}_R}{dt} = -\mathbf{u}_R - \mathbf{r}_{RL}\mathbf{i}_R ;$$

$$(15) \qquad \mathbf{u}_O = R_O\mathbf{i}_S + L_O\frac{d\mathbf{i}_S}{dt}, \qquad \mathbf{u}_S = \mathbf{u} - \mathbf{u}_O ;$$

$$(16) \qquad \frac{d\omega}{dt} = \frac{1}{J_1 + J_2}\left(M_{EM} - M_P\right) ;$$

$$(17) \qquad \frac{dQ}{dt} = \frac{1}{L_H}\left(\rho g(H_2 - H_1) + p_O - R_H Q\right),$$

$$(18) \qquad \frac{d\gamma}{dt} = \omega, \quad \frac{dQ_{k,j}}{dt} = i_{k,j}, \quad k = O, S, R, \ j = A, B, C .$$

$$(19) \qquad \mathbf{\Psi}_{SA} + \mathbf{\Psi}_{SB} + \mathbf{\Psi}_{SC} = O$$

$$(20) \qquad \mathbf{\Psi}_{RA} + \mathbf{\Psi}_{RB} + \mathbf{\Psi}_{RC} = O$$

Taking into account an algorithm of algebraic mathematical functions [1], and second equation under (15) the mathematical model of coordinates system of machine currents taking Cauchy's form is described with the following equations:

$$(21) \qquad \frac{d\mathbf{i}_S}{dt} = \left(1 + L_O\mathbf{A}_S\right)^{-1}\left(\mathbf{A}_S(\mathbf{u} - (\mathbf{r}_S + \mathbf{R}_O)\mathbf{i}_S) + \right.$$

$$\left. + \mathbf{A}_{SR}(-\mathbf{u}_R - \mathbf{\Omega}\mathbf{\Psi}_R - \mathbf{r}_{RL}\mathbf{i}_R)\right);$$

(22) $$\frac{d\mathbf{i}_R}{dt} = \mathbf{A}_{RS}(\mathbf{u} - \mathbf{u}_O - \mathbf{r}_S\mathbf{i}_S) +$$
$$+ \mathbf{A}_R(-\mathbf{u}_R - \mathbf{\Omega}\mathbf{\Psi}_R - \mathbf{r}_{RL}\mathbf{i}_R) + \mathbf{\Omega}\mathbf{i}_R,$$

where: $\mathbf{A}_S$, $\mathbf{A}_{SR}$, $\mathbf{A}_{RS}$, $\mathbf{A}_R$, – matrices, components of which depend on the main inductance and asynchronous motor dispersion, $\mathbf{\Omega}$ – matrix of asynchronous motor rotational speed [1].

Rotor cage rods voltage u_R is calculated using equations of magnetic field of one-dimensional space (coordinate – z)

(23) $$\frac{\partial H_j}{\partial t} = \frac{\nu}{\gamma_R}\frac{\partial^2 H_j}{\partial z^2}, \quad E_j = -\frac{k_u k_i}{\gamma_R}\frac{\partial H_j}{\partial z}, \quad j = A, B.$$

Taking into account boundary conditions and current flow law [1] the following is obtained:

(24) $$H_j\big|_{z=0} = \frac{i_{R,j}}{a}, \quad H_j\big|_{z=h} = 0, \quad j = A, B.$$

where: H – component of magnetic field strength vector on axis z, k_u, k_i – voltage and current transmission of the motor, ν – magnetic permeance of rotor groove wire, γ_R – electric conductivity of the rotor winding, a – groove width, $z = 0$ – groove base coordinate, $z = h$ – groove height.

By carrying out spatial discretization of equations (23) and taking into account equations (24), equations with normal Cauchy form ordinary derivatives are obtained

(25) $$\frac{dH_{j,k}}{dt} = \frac{\nu}{\gamma_R(\Delta z)^2}(H_{j,k-1} - 2H_{j,k} + H_{j,k+1}), \quad j = A, B,$$

where: k – discretization unit number, $k \geq 12$ [1].

Rotor cage rods voltage is estimated using the following equation [1]:

(26) $$u_{R,j} = -l\frac{k_u k_i}{2\gamma_R \Delta z}(-3H_{j,1} + 4H_{j,2} - H_{j,3}), \quad j = A, B.$$

where: l – groove length.

Motor starting torque is calculated using [1]:

(27) $$M_{EM} = \sqrt{3}p\,(i_{SB}i_{RA}^{\Pi} - i_{SA}i_{RB}^{\Pi})/\tau_m, \quad \tau_m = i(\psi_m)/\psi_m,$$

where: p – quantity of machine pole pairs, $^{\Pi}$ – indicates converted diagonal coordinates system [1], [4].

When analysing equation (17) it can be concluded that this very equation may be solved if virtual resistance and inductance of pump, R_H, L_H coefficients, are determined analytically. This task is a very complicated issue, however attempts to find a solution to this problem are being made. For example in publication [9] a complicated method has been presented, which method in case of transient states sometimes happens to provide results not accordant with real values. It would be great to find such solution that would enable calculation of the said coefficients by means of neural network. Our future research is going to come to this expectations. Solution to this task is going to be a method using classic characteristics of statistic relations $H = H(Q)$ for different values of pump rotation speed [2], [8].

The above is analysed for two cases:
- system presented in figure 1 pumps water from the first container to the second one (with unlimited volume), the

containers take the same level, distance between them is considerable,
- system presented in figure 1 pumps water from the first container to the second one (with unlimited volume), the containers take different levels, distance between them is considerable.

In order to create the mathematical model of a hydraulic system, results of numerical modelling are used. Vertical pump OB 16-87 is taken for analysis, the pump's head-flow curve characteristics are presented in figure 2.
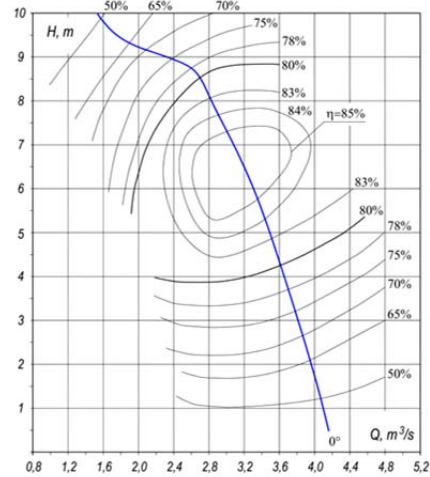
Fig.2. Head-flow curve characteristics of pump OB 16-87

One of the most significant problems regarding vertical pumps operation is their start-up and their work with nominal load. It is possible to find many publications concerning the above, for example in publication [7], using numerical methods and on the basis of turbulence model $k - \varepsilon$ and SIMPLEC algorithm, Vertical pump pressure fluctuation has been determined.

Since the analysed system is characterized by a high moment of inertia, then direct motor start-up may be a cause of pump system damage. To reduce start-up current value, an air coil of parameters R_0, L_0 (Fig.1) is used. Start-up is carried out with an open gate valve.

Bearing in mind the fact that water jets in the analysed systems are characterised by Reynolds numbers of order of magnitude 10^6 [8], parabolic relation of hydraulic flow rate in pipeline is adopted. In such case pipeline equation is as follows:

(28) $$H_p = H_g + S_p Q^2,$$

where: H_g – geometrical liquid head,
S_p – pipeline hydraulic resistance.

Pipeline hydraulic resistance is [8]:

(29) $$S_p = \frac{8(\lambda L_p / D_p + \Sigma\zeta)}{\pi^2 g D_p^4},$$

where: L_p, D_p – length and internal diameter of pipeline, λ, $\Sigma\zeta$ – hydraulic friction coefficient and sum of local hydraulic resistances.

In the least complicated case, when liquid head is $H_g = 0$ (26), torque M_P relation is determined analytically on an pump shaft in the function of rotational speed – ω:

(30) $$M_P = \frac{\rho g S_p Q_o^3}{\eta_o \omega_o^3}\omega^2,$$

where: ρ – liquid density; Q_o, η_o, ω_o – flow rate, pump efficiency and nominal rotation speed.

In the case when $H_g > 0$ the problem has been solved using numerical methods. Numerical modelling results are presented for pump OB 16-67 and steel pipeline of diameter $D = 1200$ mm and length $L = 500$ m, for different liquid head values $H_g = 2$ m and $H_g = 4$ m. Adapted thickness of pipeline wall is $- \Delta_e = 1$ mm, the unevenness taken into account, sum of all coefficients of pipeline resistance is $\Sigma\zeta = 1,75$.

Liquid head H_0 when rotation speed $n < n_o$ is calculated using the following equations:

$$(31) \qquad Q = (n/n_o)Q_o \,; \; H = (n/n_o)^2 H_o \,,$$

where: Q_o – pump flow rate at nominal speed n_o.

Characteristics of liquid head for pump OB 16-87 have been approximated using the following parabolic relations:

$$(32) \qquad H_p = a + bQ + cQ^2 \,,$$

where: a, b, c − coefficients, dependent from n speed, estimated using least squares method [8].

Values of the said coefficients are presented in table 1.
Table 1.

Speed n rotation/min	Parabolic coefficients		
	a	b	c
585	5.599	5.268	-1.56
550	4.949	4.953	-1.56
500	4.09	4.502	-1.56
450	3.313	4.052	-1.56
400	2.618	3.602	-1.56
350	2.004	3.152	-1.56
300	1.473	2.702	-1.56
200	0.655	1.801	-1.56
100	0.164	0.901	-1.56

Relations of efficiency, liquid head and pump in function of flow rate are presented in figure 3. Characteristics 1-7 are carried out for the following rotational speed values: 585, 550, 500, 450, 400, 350 and 300 rotations/min; characteristics 8, 9, 10 present liquid head respectively: $H_g = 0$ m; $H_g = 2$ m; $H_g = 4$ m; and characteristic 11 presents pump efficiency.

Working points coordinates $(Q; H)$ for each rotational speed n have been calculated numerically, using system of equations (28) and (32), for respective values of coefficients a, b, c specified in table 1.

Pump efficiency η' for speed $n < n_o$ when $H_g > 0$ differs from value η_o. Recalculation of efficiency values was carried out using states similarity method:

$$(33) \qquad H_i = H_o (Q_i / Q_o)^2 \,,$$
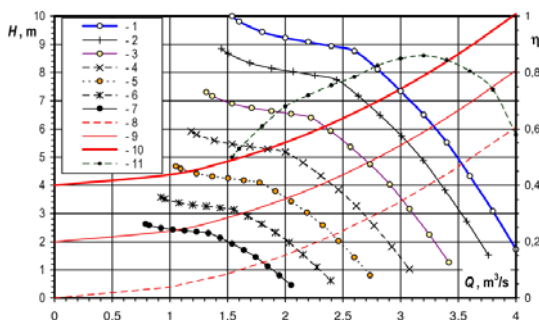
Fig.3. Characteristics of efficiency, liquid head and vertical pump in the function of flow rate

Solving equations (32) and (33) in relation to Q_i for coefficients a_i, b_i, c_i, which correspond to speeds n_i results with finding drive motor torque load:

$$(34) \qquad M = \frac{30\rho g Q H}{\pi n \eta'} \,.$$

Relation between rotation torque of pump shaft M_P and angular velocity ω was approximated using the least squares method (Fig.4). It has been assumed that it is possible to extrapolate the obtained trend lines including velocities $\omega \to 0$.
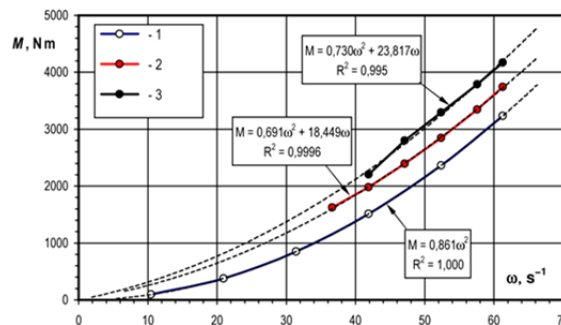
Fig.4. Graphic relations of rotation torque of shaft of pump OB 16-87 in the function of angular velocity for a pipeline (D=1,2 m, L=500 m): 1 − H_g=0 m; 2 − H_g=2 m; 3 − H_g=4 m

System of differential equations: (16), (18), (21) − (23), (25) is subjected to integration upon solving equations (15), (24), (26), (27), (30), (32), (34).

Computer simulation results
The presented mathematical model was used to analyse transient states of drive system presented in figure 1. Since nominal angular velocity of the motor is $\omega_n = 740$ rotations/min., and of pump − $\omega_P = 585$ rotations/min. then the system in figure 1 is provided with gear characterized by coefficient $k_T = 750/585$. For computer simulations motor 12-52-8A was used, which motor is characterized with the following nominal values: $P_n = 320$ kW; $U_n = 6$ kV; $I_n = 39$ A; $\omega_n = 740$ s^{-1}, $p = 4$, $J_R = 49$ kgm^2, and parameters: $r_S = 1,27$ Ω, $R_{RL} = 0,21$ Ω, $\alpha_S = 38,9$ H^{-1}, $\alpha_{RL} = 70$ H^{-1}, $h = 0,038$ m, $l = 0,23$ m, $a = 0,005$ m, $J_\Sigma = 49$ kgm^2. Motor magnetization curve is approximated using the following equation: $\Psi_m = 12,4$ arctg $(0,066\, i_m)$. Air coil parameters are as follows $R_O = 1,2$ Ω, $L_O = 30$ mH.

System of differential equations (16), (18), (21) − (23), (24) is integrated by Runge-Kutt method of 4th order.

In the course of this task three simulations are carried out for different liquid heads: 1 − $H_g = 0$ m; 2 − $H_g = 2$ m; 3 − $H_g = 4$ m.

At moment of time $t = 0$ s, the system presented in figure 1 was powered from power grid with voltage u. At steady state the supply voltage got disconnected after time interval $t = 5$ s. The experiment took 16 s.

Figure 5 presents instantaneous rotation speeds of the drive system for three liquid heads: 1, 2, 3.

Dynamic properties of the system differ depending on the liquid head. Overrun for zero liquid head takes the longest. The higher the liquid head the shorter the overrun, this is due to the fact that liquid hear rise requires use of potential energy, which energy upon being transferred into kinetic energy causes faster motor stopping.

In figure 6 load torque of asynchronous motor is presented for different liquid head values: 1 − $H_g = 0$ m; 2 − $H_g = 2$ m; 3 − $H_g = 4$ m.
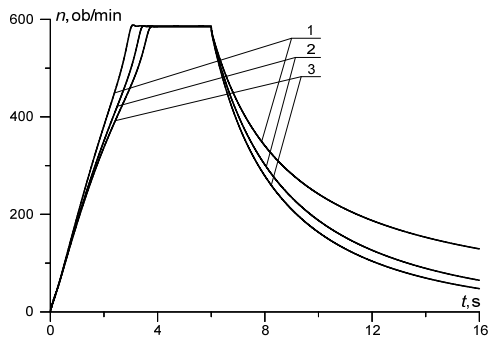
Fig.5. Instantaneous rotational speeds for hydraulic drive
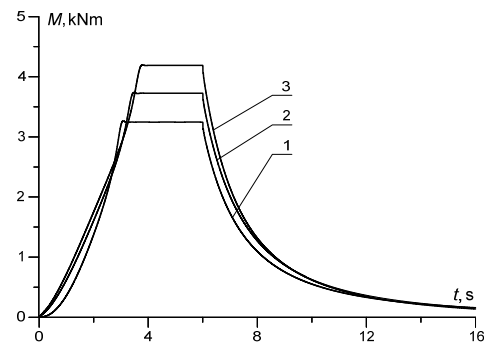
Fig.6. Instantaneous load torques

Figures 7, 8 present instantaneous currents of stator phase A and calculated current of phase A of rotor, for H_g = 4 m. Drive start-up took about 4 s. Within this time the highest current values were obtained. Upon start-up end, current was characterized by steady state, it took nominal value. After about 5 s. when in overrun state the rotor currents values equal zero.
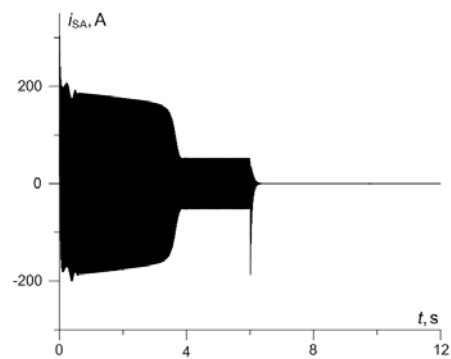
Fig.7. Instantaneous current of stator phase A
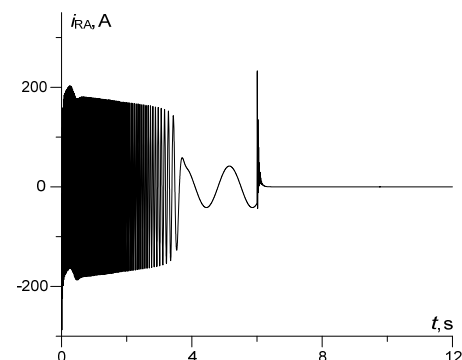
Fig.8. Instantaneous calculated current of phase A of rotor

Figure 9 presents instantaneous phase voltage of phase A for H_g = 4 m. Stator featuring air coil favours reduction of voltage occurring during drive start-up. In steady state the voltage was close to a nominal value.
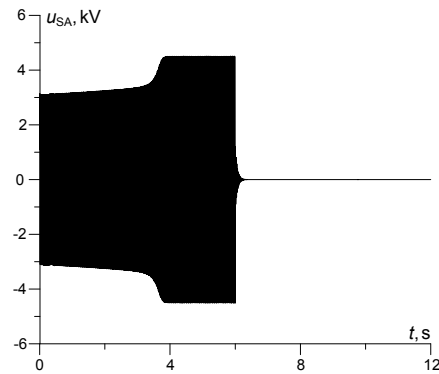
Fig.9. Instantaneous phase voltage of stator phase A
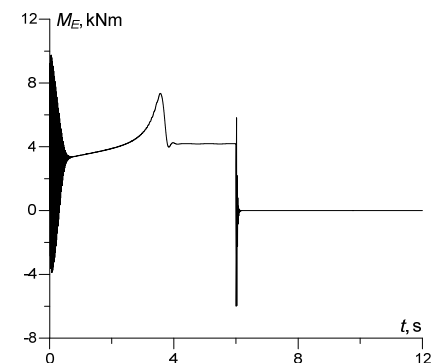
Fig.10. Instantaneous electromagnetic torque of asynchronous motor

Figure 10 presents instantaneous electromagnetic torque of asynchronous motor for H_g = 4 m. It should be noted that upon switching the voltage off, torque changes significantly which affects operation of gear mechanism and pump. To reduce such great mechanical tensions in drive system it is necessary to use flexible clutch, which is going to be a subject the studies in the future.
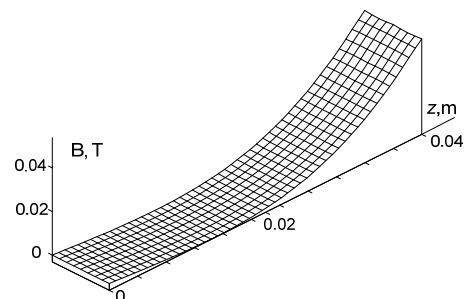
Fig.11. Spatial distribution of magnetic induction in rotor cage rod for H_g = 4 m within time interval t = 0.1 s
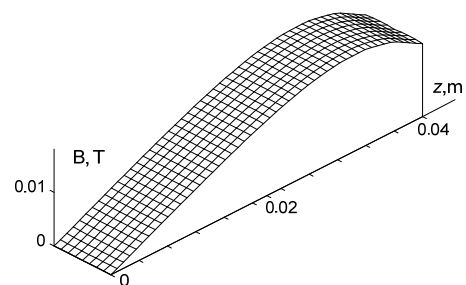
Fig.12. Spatial distribution of magnetic induction in rotor cage rod for H_g = 4 m within time interval t = 2 s
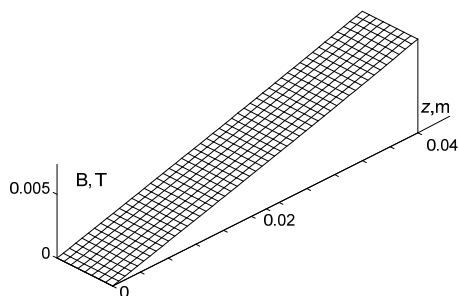
Fig.13. Spatial distribution of magnetic induction in rotor cage rod for H_g = 4 m within time interval t = 5 s

Figures (11 – 13) present spatial distributions of magnetic induction in rotor cage within the following time intervals: t = 0.1 s, t = 2 s i t = 5 s. Influence of displacement of current in groove wires is clearly visible. At start-up, maximum current density occurs at top part of the groove and maximum amplitude can be observed for electromagnetic wave (Fig. 11). After start-up the wave penetrates groove, wave amplitude reduces (Fig. 12). In figure 13, when the wave changes with frequency of about 1 – 2 Hz (Fig. 8) it is characterized with minimum amplitude, and current density throughout the whole groove is close to the linear course – current displacement is practically unnoticeable.

Conclusions
1. The use of interdisciplinary variation approach in mathematical modelling of complex electrodynamics systems featuring subsystems referring to different science fields greatly expands scope of analysed system. Additionally this guarantees obtained results reliability.
2. The use of similarity theory in hydraulic systems allowed to present analytical relations of pump drive load in the function of rotational speed in dynamic states. The said approach significantly expands analysis of operation of electrohydraulic drives within vast scope of operation.
3. On the basis of computer simulation results the following conclusions are made:
   a) few meters high increase of liquid head in relation to hundreds of metres of horizontal pipeline length significantly influences pump load torque value;
   b) including air coil into motor stator circuit significantly reduces start torque. This solution reduces shock torques occurring in transient states;
   c) in pump systems with frequent start-ups, connection of motor with pump must be carried out using flexible clutch, which reduces shock torque on motor shaft, gear and pump;
   d) spatial dispersion of magnetic field strength shows real complex processes of displacement of rotor grooves current.

Authors: *prof. dr hab. inż. Zbigniew Łukasik UTH Radom, Wydział Transportu i Elektrotechniki, ul. Malczewskiego 29, 26-600 Radom, E-mail: z.lukasik@uthrad.pl; dr hab. inż. Andriy Czaban prof. nadzw. UTH Radom, Wydział Transportu i Elektrotechniki, ul. Malczewskiego 29, 26-600 Radom, E-mail: atchaban@gmail.com; dr inż. Andrzej Szafraniec UTH Radom, Wydział Transportu i Elektrotechniki, ul. Malczewskiego 29, 26-600 Radom, E-mail: a.szafraniec@uthrad.pl; dr inż. Vołodymyr Żuk, Narodowy Uniwersytet "Politechnika Lwowska", E-mail: zhuk_vm@ukr.net.*

REFERENCES
[1] Czaban A., Zasada Hamiltona-Ostrogradskiego w układach elektromechanicznych, Lwów (2015), *Wydawnictwo T. Soroki*, 464
[2] Jędral W., Pompy wirowe odśrodkowe, *Oficyna Wydawnicza Politechniki Warszawskiej*, (1996), 324
[3] Domek S., Zintegrowany system monitorowania warunków pracy układu napędowego obrabiarki sterowanej numerycznie, *Przegląd Elektrotechniczny*, 86 (2010), nr 6, 113-115
[4] Czaban A., Lis M., Klatow K., Patro M., Gastołek A., Model matematyczny układu energetycznego składającego się z transformatora mocy, linii długiej oraz obciążenia RLC, *Przegląd Elektrotechniczny*, 93 nr (2017), nr 1, 133-136
[5] Kalenyuk P.I., Nytrebych Z.M., On an operational method of solving initial-value problems for partial differential equations induced by generalized separation of variables, *Journal of Mathematical Sciences*, Vol. 97, (1999), 3879-3887
[6] White D.C., Woodson H.H., Electromagnetic Energy Conversion, *John Wiley & Sons Inc, New-York* (1958)
[7] Zhang D., Shi W., Chen B., Guan X., Unsteady flow analysis and experimental investigation of axial-flow pump, *Journal of Hydrodynamics*, (2010), V. 22(1), 35−43
[8] Mandrus W., Żuk W., Hydraulika, napędy hydrauliczne i pneumatyczne maszyn wojskowych, Lwów, *ACB*, (2013), 372
[9] Костышин В., Моделирование центробежных насосов на основании электрогидравличиской аналогии, *Ивано-Франковск*, (2000), 163
[10] Szafraniec A., Sterowanie optymalne wielosilnikowych układów napędowych w systemach transportowych i przemysłowych, *Zeszyty Naukowe Syberyjskiej Akademii Samochodowej* nr T08D07/2003/8, Omsk (2003), 16-19
[11] Lis M., Modelowanie matematyczne procesów nieustalonych w wielomaszynowym układzie napędowym o złożonej transmisji ruchu, *Przegląd Elektrotechniczny*, 92 (2016), nr 12, 253-256